Available online www.jocpr.com

Journal of Chemical and Pharmaceutical Research, 2015, 7(6):470-487

Research Article

ISSN : 0975-7384
CODEN(USA) : JCPRC5

Evaluation of cytotoxic effect of metallic nanoparticles in an *in vitro* liver cancer model

Samah A. Loutfy[1], Rokaya H. Shalaby[2], Ahmed R. Hamed[3], Mona B. Mohamed[4], Ahmed Barakat[5], Zeinab F. Abdullah[1], Hend Yousef[6], Alaa Tamim[7], Hoda E. Eldin[2] and Noha M. Hegazy[7]

[1]*Virology and Immunology Unit, Cancer Biology Department, National Cancer Institute, Cairo University, Cairo, Egypt*
[2]*Zoology Department, Faculty of Women for Arts, Science and Education, Ain Shams University*
[3]*Pharmaceutical Research Group, Centre of Excellence for Advanced Sciences, National Research Centre, El-Buhoos st. (formerly El-Tahrir), Dokki, Giza, Cairo, Egypt*
[4]*Photochemistry & Photobiology, LAMPA, National Institute of Laser Enhanced Sciences, Cairo University, Cairo, Egypt*
[5]*Microbiology Department, Faculty of Science, Ain Shams University, Cairo, Egypt*
[6]*Pathology Department, National Cancer Institute, Cairo University, Cairo, Egypt*
[7]*Department of Environment and Occupational Medicine, National Research Center, El-Buhoos st. (formerly El-Tahrir), Dokki, Giza, Cairo, Egypt*

ABSTRACT

We aim to evaluate cytotoxic effect of silver and gold metallic nanoparticles (AgNPs & AuNPs) on human cucasian hepatocellular carcinoma cell line model (HepG2) and their possible anti-proliferative activity. This new class of engineered nanoparticles with desired physicochemical properties can be applied as new therapeutic approaches against human liver cancer disease. HepG2 was used as a model of human liver cancer cells. Metallic nanoparticles were characterized using UV-visible spectra and transmission electron microscopy (TEM). Cytotoxic effects of metallic nanoparticles on HepG2 cells were followed by colorimetric neutral red and SRB cell viability assays. Further investigation of cytotoxic effect of our nanomaterials were further investigated on a cellular and molecular level using cell cycle analysis , DNA and some apoptotic genes expression on a level of mRNA for P53, Bak, Bax, BCl_2 and β actin was served as housekeeping gene. Treatment of HepG2 with different concentrations of 22 nm diameter of AgNPs did not show alteration of cell morphology after 24 h of cell exposure. Also, when cells were treated with high concentration of AgNPs (viability was 78% after cell treatment with 10 µM and decreased to 46% after treatment of cells with 1000 µM). Cellular evaluation of AgNPs revealed progressive accumulation in the S phase of the cell cycle correlating with decreased number of cells in the G2/M phase followed by cellular DNA fragmentation. Extensive evaluation of cytotoxic effect of AgNPs showed mRNA apoptotic genes expression (P53, Bak, Bax, BCl_2) without expression of mRNA of caspase 3 gene which was expressed in untreated cells, suggesting involvement of intrinsic apoptotic caspase independent pathway. Treatment of HepG-2 with different concentrations of 34 nm diameter of AuNPs did not show alteration of cell morphology after 24 h of cell exposure. Such metallic nanoparticles did not reveal toxic effect at concentration up to 50 µM after 48 h of cell exposure. Cellular evaluation of AuNPs revealed progressive accumulation at G0/G1and at G2/M phases of cell cycle. Also the same results were obtained by treating cells with AgNPs, where the expression of mRNA of P53, Bak, Bax, BCl_2 without expression of mRNA of caspase 3 gene was observed in treated cells, suggesting intrinsic apoptotic caspase independent mechanism but may be induced by different molecules than that exerted by AgNPs. Our engineered silver nanoparticles at size of 22nm revealed genotoxic effect on human liver carcinoma cell line HepG-2 through intrinsic apoptotic caspase independent mechanisms. Further quantitative analysis and investigation of impact of time on genotoxic effect are required before reaching a final conclusion and starting in vivo assays.

Key words: Metallic nanoparticles, anti-proliferative activity, HepG2, apoptotic genes expression

---

INTRODUCTION

Hepatocellular carcinoma (HCC) is the sixth most common and the third most fatal cancer in the world, with 782,000 new cases occurring and 746,000 deaths in 2012 worldwide. The distribution of HCC varies geographically, and is related to the prevalence of hepatotropic virus [1]. In Egypt, hepatocellular carcinoma (HCC) is the most common type of cancer, dramatically increased in the last few years making it the 4th in ranking among all types of cancer, and the second only in males after carcinoma of the urinary bladder [2].

The increase in incidence of HCC among Egyptian population parallels the marked increase in incidence of HCV infection which is expected to at least double in the next 20 years [3]. However, there are many strategies available for treatment of HCC [3]. All present modalities are very expensive and time consuming. Therefore other treatment modalities are required for managing such aggressive type of cancer.

In the last two decades, a number of nanoparticle-based therapeutic and diagnostic agents have been developed for the treatment of cancer, diabetes, pain, asthma, allergy, infections, among others [4].

Metallic nanoparticles are known as plasmonic materials; they have a marked ability to absorb and scatter light at a frequency that is resonant with their surface plasmon oscillation. This resonance frequency depends on particle shape, size, and the density of the particle's electron distribution and the surrounding dielectric environment. Thus, it provides very useful information regarding particle properties.

Several reports have demonstrated antiproliferative activity of metallic nanoparticles against different types of human cancers. There is a need for extensive evaluation of the mechanism underlying cell death via investigating some apoptotic genes expression in response to cell treatment with metallic nanommaterials [5,6,7]. It has been demonstrated that the oxidative stress paradigm of nanomaterials that induces cell death is linked to intrinsic apoptotic network [8]. Therefore, the aim of the current study is to investigate some of apoptotic genes expression in response to metallic nanoparticles that may linked to their anti- proliferative activities against human liver cancer cells (HepG2). This will encourage further exploitation studies in vivo assay as a newer therapeutic approach against one of the commonest cancer diseases among Egyptian population.

EXPERIMENTAL SECTION

Preparation and characterization of silver nanoparticles

Spherical silver nanoparticles (AgNPs) were synthesized in an aqueous medium by the chemical reduction of AgNO3 [9] with minor modification. The reduction used NaBH4 as the reducing agent while sodium citrate and polyvinyl pyrrolidone (PVP) served as capping materials to prevent aggregation and excessive growth of the nascent particles. A mixture of 3x10-4 MM of tri-sodium citrate and 0.2 g PVP was dissolved in 10 ml distilled water and mixed well, with stirring. A 100 mL volume of 10-3M AgNO3 solution was added to the stirred solution. Then, 0.5 mL of aqueous solution of 1x10-3M NaBH4 was added drop by drop. The color of the solution changed from colorless to yellow. UV-VIS absorption spectra were recorded (Perkin-Elmer Lambda 40 spectrophotometer) using 1 cm matched quartz cells.

Nanoparticle parameters

Particle size, shape and size distribution profile were determined using the transmission electron microscopy (TEM) (Nanotech. Company for Photo-Electronic, Dreamland, 6-October). A drop from a very dilute sample solution was deposited on an amorphous carbon-coated copper grid and left to evaporate at room temperature. Imaging was accomplished using a Joel JEM-2100 microscope (accelerating voltage 200kV; Gatan Erlangshen ES500digital camera) [10].

Preparation and characterization of gold nanoparticles

Spherical gold nanoparticles (AuNPs) were chemically prepared by the citrate reduction of HAuCl4.3H2O where sodium citrate serving as a capping material to prevent aggregation and further growth of the particles [11]. Tri-sodium citrate (0.0388 M, 10 mL) was added quickly to a boiling HAuCl4 solution (1x10-3 M, 100 mL). The color of the solution changed from yellow to colorless and finally to wine red which was considered as an indication of the formation of AuNPs. The solution was then refluxed for an additional 15 min, then the heater was turned off and the solution was stirred until it reached room temperature to control the particle size and thus achieving a narrow particle size distribution. The absorption spectrum of the obtained sample was measured via UV-VIS spectrophotometer, and the particle shape and size were characterized using TEM.

Nanoparticle parameters

Particle size, shape and size distribution profile were determined using the transmission electron microscopy (TEM) (Nanotech Company for Photo-Electronic, Dreamland, 6-October, Egypt). A drop from a very dilute sample solution was deposited on an amorphous carbon-coated copper grid and left to evaporate at room temperature. Imaging was accomplished using a Joel JEM-2100 microscope (accelerating voltage 200 kV; Gatan Erlangshen ES500 digital camera) [12].

Cell Culture

Human liver cancer cell line (HepG2) and normal fibroblast cell line (WISH) were obtained from American Tissue Culture Collection (ATCC), USA. The Cells were cultured and maintained in RPMI 1640 media(Biowest) supplemented with 10% fetal bovine serum (Biowest), and antibiotics (2% penicillin-streptomycin (100 IU/ml), and 0.5% fungizone (Biowest).The cells were maintained in monolayer culture at 37oC under a humidified atmosphere of 5% CO2. The cells were sub-cultured by trypsinization (0.025% trypsin and 0.0025% EDTA; Biowest), and maintained in tissue culture laboratory at the National Cancer Institute, Cairo University, Egypt with cryogenic banking of low-passage cells to maintain uniformity of cell properties through the study [13]. Cell numbers and viability were monitored by standard Trypan blue dye exclusion procedures. Growth curves for HepG2 and WISH were determined under baseline conditions prior to investigation of cytotoxicity.

Cell culture and treatment with metallic nanoparticles (AgNPs & AuNPs)

All our metallic nanomaterials were sterilized under UV irradiation for 3 hours before their application in tissue culture. Serial dilutions were prepared in 2% RPMI 1640 giving AuNPs concentrations 100, 50, 25, 12 and 6uM. Cytotoxicity was investigated through measurement of cell viability using Sulforhodamine B assay [14]. Positive and negative cytotoxicity controls were run in each plate. Negative controls (cells with media only; untreated cells), were set as 100% viability. Cells subjected to osmotic shock (treated with distilled water) were taken as positive controls (zero viability) were used to subtract background from all OD values. Morphological changes of cells were followed by phase contrast microscopy (40x magnifications). Neutral red colorimetric assay [15] was performed to investigate cytotoxic effect of AgNPs according to our previous report [16], cells were treated with different concentrations of AgNPs at different time intervals 24 h,48 h and72 h. The percent of viability was estimated based on the following equation:

$$\% \text{ viability} = \frac{\text{(mean OD of test sample)}}{\text{(mean OD of negative control)}} \times 100$$

Sulforhodamine B (SRB) assay

The cytotoxicity of the nanomaterials was tested against HepG-2 cells and WISH cells by SRB assay. Exponentially growing cells were collected using 0.25% Trypsin-EDTA and plated in 96-well plates at 1000-2000 cells/well. Cells were exposed to nanoparticles for 72 h and subsequently fixed with 10% TCA (Trichloroacetic acid, Sigma–Aldrich, UK) for 1 h at 4 ºC. After several washings with PBS, cells were exposed to 0.4% SRB solution for 10 min in a dark place and subsequently washed with 1% glacial acetic acid. After drying overnight, Tris-HCl was used to dissolve the SRB-stained cells and color intensity was measured at 540 nm wavelength using micro plate reader (Biotek Model: ELX 800, USA) [14].

Flow cytometric cell cycle analysis

HepG2 cells (5x105cells/well) were plated in 6-well microplates. After treatment with IC50 concentration of metallic nanoparticles (AgNPs & AuNPs), cells were washed twice with PBS, suspended in 300µl of PBS (pH 7.3), and finally fixed with 4ml of ice-cold 70% ethanol. To stain with propidium iodide (PI), Cells sedimentation was performed by centrifugation, the ethanol was removed and cells washed once with PBS. The cell pellets were then resuspended in 1ml of PI/Triton X-100 staining solution (0.1% Triton X-100 in PBS, 0.2 mg/ml RNase A, and10mg/ml PI) and incubated for 30 minutes at room temperature. The stained cells were analyzed using a MoFlo flow cytometer (Dako Cytomation, Glostrup) to calculate the percentages of cells occupying the different phases of the cell cycle [17].

Imaging of cellular uptake of metallic nanoparticles (AgNPs & AuNPs)

HepG2 and WISH cells were treated with 100 µM of AgNPs or AuNPs for 24 h. Cells were washed with PBS buffer then fixed with 2% glutaraldehyde for 2 hours and washed twice with PBS before fixation in 1% OsO4 for 1hour. Following agarose (1.5%) enrobing, Spurr's resin embedding, and ultrathin (50 nm) sectioning, the samples were stained with 2% aqueous uranyl acetate and 25 mg/mL lead citrate and imaged with a JEOL 100S electron microscope [18].

DNA fragmentation

Fragmentation of cellular DNA was investigated following treatment of MCF-7 cells with AgNPs at low and high concentrations (10 µM and 100 µM, IC50 respectively) compared to estimated IC50. But DNA fragmentation was investigated following treatment of MCF-7 cells with AuNPs at low and high concentrations (10 µM and 100 µM, IC50 respectively) compared to estimated IC50. A fixed amount (100 ng) of cellular DNA (Genomic DNA Purification Kit, Amersham Biosciences) extracted from treated and untreated cells was subjected to 1.5% agarose gel electrophoresis in Tris-acetate buffer pH 8.2, stained with 0.5 µg/ml ethidium bromide. The bands were examined under UV transillumination and photographed. Smearing, or presence of many low molecular weight DNA fragments, is a characteristic feature of apoptotic cells [19].

Detection of cellular apoptotic genes expression by One-Step Reverse transcription polymerase chain reaction (RT-PCR)

Apoptotic signaling genes include; P53, Bak , Bax and Caspase 3 were detected by In- house RT –PCR assay. The housekeeping β-actin gene was used as internal control. This was optimized according to protocol of Gopinath and colleagues [20] which included:

a. Isolation of cellular RNA

Total RNA Total RNA was isolated from treated and untreated cells using QIAamp RNA Blood Mini Kits (QIAgen, USA) according to manufacturer's instructions. Then total RNA extracts were placed on ice and used immediately for RT-PCR or stored at -40oC until analysis. The amount of cellular RNA was measured by spectrophtometry using a Nano-Drop 2000 spectrophotometer (Thermo Scientific/US, Canada) and 500ng of RNA template was used in the RT-PCR assays.

b.Amplification of cellular RNA

This step was performed using QIAGEN One Step RT-PCR Kit (USA) that contains a mixture of three enzymes, two engineered reverse transcriptases and a hot start Taq DNA polymerase. This kit allows both reverse transcription and subsequent amplification of the cDNA produced in the same tube in one step; this avoids the risk of carryover contamination. The extracted RNA (500ng/reaction) was included in the reaction mixture containing 5x PCR buffer (Qiagen), 5x Q- solution, 200 µ M dNTPs, 1µ1 of enzyme mixture (Qiagen) along with 0.6 µM of gene specific upstream and downstream primers according to previous prorocol [20], in a final volume of 25 µl in Gene Amp PCR system 9700 (Applied Biosystems, USA). The samples were overlaid with mineral oil to prevent evaporation. First cycle is 37oC for 50 min to convert all RNA into cDNA followed by inactivating enzyme at 95oC for 10 min , then this was followed by amplifying program include: Initial denaturation at 94oC for 2 min, followed by 35 PCR cycles of denaturation at 94oC for 15 s, annealing at 55 ◦C for 30 s, extension at 68 ◦C for 1min with a final extension at 68◦C for 5min.

c. detection of PCR product by agarose gel electrophoresis

Fifteen µl of PCR product was subjected to electrophoresis on a 1.5% agarose gel (Sigma) in 1X Tris-Acetate buffer (TAE) pH 8.2, stained with 0.5ug /ml ethidium bromide. After electrophoresis, the gel was examined under UV transilluminator and photographed. Gene expression was quantified based on the band intensity measured by image software and the expression of reference gene ß-actin was considered 100%.

RESULTS

1. Silver nanoparticles (AgNPs)

Following reflux, the silver nitrate solution appeared yellow; inspection of the uv-visible spectrum revealed a peak at 405 nm characteristic of small-diameter AgNPs, Figure 1A. A representative TEM image of the AgNPs, (Figure 1B) demonstrates the presence of approximately spherical particles, although a few prismatic fragments were also present. The zeta size of AgNPs used in this study was 22nm as shown in Figure 1C. The zeta potential of AgNPs was found to be -9.45 mV as illustrated in Figure 1D.

2. Gold nanoparticles (AuNPs)

The visible absorption spectra of the wine red colloidal AuNPs showed a well-defined absorption band at λmax=522 nm (Figure 2A), Figure 2B demonstrates TEM image of spherical AuNPs. The zeta size of AuNPs used in this study is 36nm as shown in Figure 2C. Zeta potential of AuNPs was found to be -33.6mV, this could be due to negative charges of the citrate capping agent (Figure 2D).

Interaction of metallic nanoparticles (AgNPs & AuNPs) with HepG2 cells

Light microscopy

HepG2 cells treated with 100 µM AgNPs for 24 h (Figure 3A a) did not show profound morphological changes and hence did not reveal any characteristic of cytotoxicity, also, treatment with 10 µM AgNPs (Figure 3A b) demonstrated no significant differences compared to control cells.

HepG2 cells treated with 100 µM AuNPs or with 10µM for 24 h (Figure 3B a) did not show profound morphological changes as well, hence didn't reveal any characteristics of cytotoxicity (Figure 3B b).

Transmission electron microscopy

Transmission electron microscopy (TEM) images demonstrated binding and internalization of silver nanoparticles in HepG2 cells. Aggregation of AgNPs to form nanoparticle clusters on the cell membrane is evident (Figure 4A). Examination of images at higher magnification shows intracellular nanoparticle clusters, mainly associated with membranes, with most of the dispersed nanoparticles in the cytoplasm. Treatment with AgNPs is associated with disruption and fragmentation of intracellular organelles; localization of AgNPs into the nucleus and nuclear membrane is also apparent.

Figure 4B demonstrated internalization of gold nanoparticles in HepG 2 cells. It was observed to be internalized into cytoplasm, nucleus and into mitochondria

Cytotoxic effect of metallic nanoparticles (AgNPs & AuNPs) in HepG-2 cells

The cytotoxic effect of various concentrations of silver nanoparticles (10 µM, 100 µM, 1000 µM) was assessed in HepG2 cell cultures using Neutral red colorimetric assay at different time intervals; 24 h, 48 h, 72 h. Results showed that cytotoxic effect increased when cells treated with high concentration of AgNPs (viability was 78% after cell treatment with 10 µM and decreased to 46% after treatment of cells with 1000 µM).

Regarding cytotoxic effect of gold nanoparticles (100, 50, 25, 12 and 6 µM), our results showed that our engineered metallic gold nanoparticles was safe up to a final concentration of 50 µM after 48 h of cell exposure.

Effect of metallic nanoparticles (AgNPs & AuNPs) on the cell cycle

The nature of AgNPs action was further investigated by flow cytometric analysis of cell cycle and DNA contents of cells treated with 10 µM or 1 mg/L of AgNPs for 24 h. Untreated cells showed the expected cell cycle pattern for continuously growing cells, whereas treated cells showed a progressive accumulation in the S phase of the cell cycle correlating with decreased number of cells in the G2/M phase.

Regarding the effect of AuNPs on cell cycle, treatment of HepG2 at concentration of 100 µM for 24 h didn't show that toxic effect exerted by AgNPs, but in contrast it affected cell proliferation as evidenced by cell accumulation at G2/M phase (8.5% for AuNPs versus 3% for AgNPs). Table3, Figure 6.

DNA fragmentation of metallic nanoparticles (AgNPs & AuNPs)

DNA fragmentation analysis was carried out to investigate the toxic effects of AgNPs on cell stability and DNA replication. DNA fragmentation characteristics of late apoptosis was observed after treatment of cells with a high concentration of AgNPs (100 µM), while much less significant changes were seen when the AgNPs concentration was reduced to 10 µM. DNA fragmentation was not observed in untreated cells (cell control); as shown in Table 4, Figure 7A). These results explain our previous results of flow cytometric analysis and accumulation of cells in S phase.

Regarding effect of AuNPs on cell stability and proliferation investigated in parallel to the effects of AgNPs. DNA fragmentation characteristic of apoptotic effect was observed after treatment of cells with high concentration of AuNPs (100µM, 35.8mg/L), while much less toxic effect was seen when the AuNPs concentration was reduced to 10 µM compared to untreated cells, as shown in Table 5, Figure 7B).

Apoptotic genes expression as detected by One-Step RT PCR

Extensive evaluation of cytotoxic effect of metallic nanoparticles on expression of apoptotic genes (P53, Bak, Bax, BCl2 and caspase 3) at a transcriptional level using One-Step RT PCR was performed after treatment of HepG2 with each of AgNPs and AuNPs at concentration of 100 µM for 24 h. β-actin house keeping gene was detected in each run to ensure RNA integrity. Our results showed that all selected genes were expressed in untreated HepG2 cells but cells treated with metallic nanoparticles showed expression of P53, Bak, Bax, BCl2 but didn't show expression of caspase 3 .Results are shown in Figure 8(A,B,C,D,E,F)

Table 1. Comparison between the cytotoxic effect of different concentrations of AgNPs (10, 100, 1000µM) on HepG-2 cells after 24,48, 72 h of cells exposure by neutral red assay

Exposure time (h)	24	48	72
IC50	899.3	111.2	65.48

Table 2.Comparison between the cytotoxic effect of AuNPs on HepG-2 and Wish cells, viability (%) in the concentration rang (0-100µM) for 48hrs incubation period

(Conc (µM	AuNPs on HepG2 (48hrs)		AuNPs on Wish (hrs48)	
	O.D	%Viabl	O.D	%Viabl
0	1	100	1	100
6.25	1.016	101	1.02	102
12.5	**0.894**	**89.4**	**1.07**	**107**
25	0.813	81.3	1.2	120
50	0.894	89.4	0.99	99
100	0.75	75	0.96	96

Table 3. Flow cytometric analysis of effect of 50uM of AgNPs and AuNPs

	% G0-G1	% G2-M	% G2/G1-Phase	% S phase	Diploid
Control of AgNPs	65.14	6.78	1.91	28.08	0.12
AgNPs	52.12	3.05	1.94	44.83	0.01
Control of AuNPs	65.14	6.78	1.91	28.08	0.12
AuNPs	70.52	8.54	1.91	20.94	0.01

Figure (1A) Characterization of silver nanoparticle preparation. UV-visible spectrum

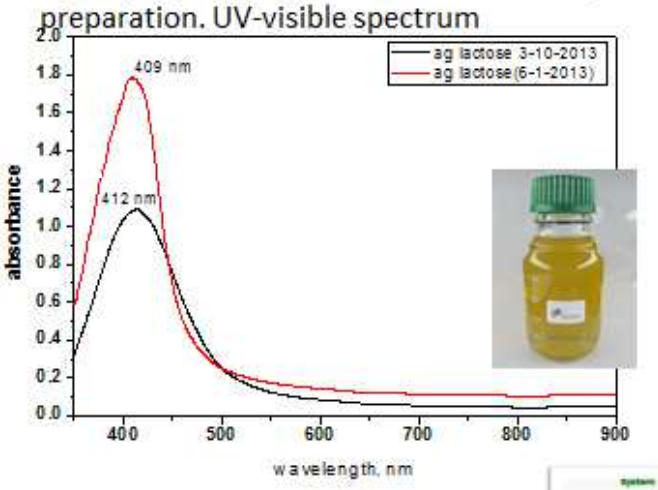

Figure(1B) Characterization of silver nanoparticle preparation. (Transmission electron microscope (TEM)image

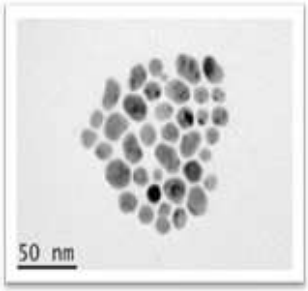

Figure 1C. Zeta size of silver nanoparticle

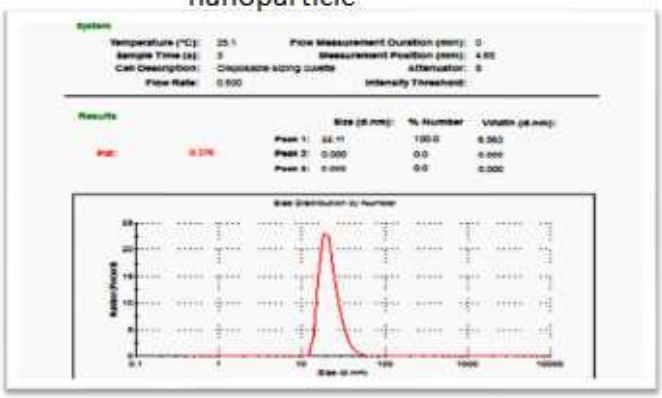

Figure 2A The UV-Vis spectrum of gold nanoparticles

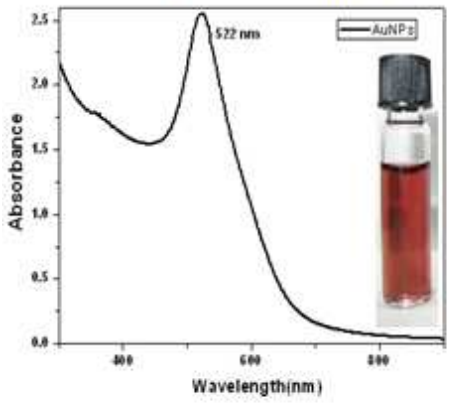

Figure 2B. TEM of gold nanoparticles

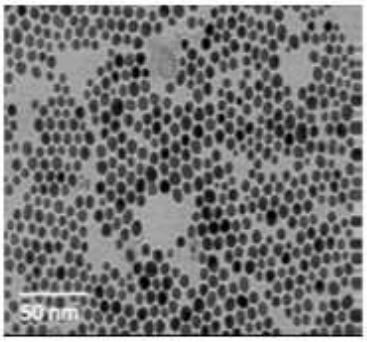

Figure 2C. Zeta size of Gold nanoparticles

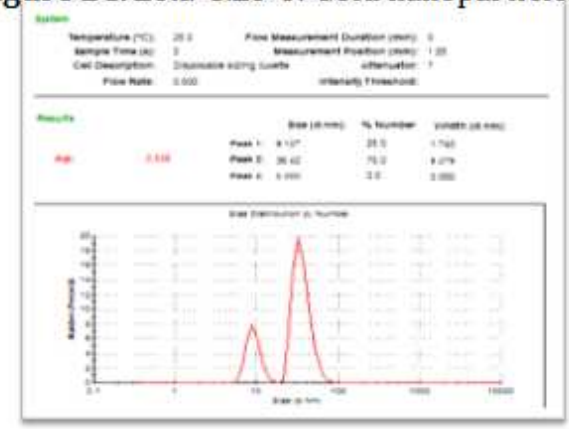

Figure (3A) HepG2 control. Light microscopy (phase contrast, 40x)

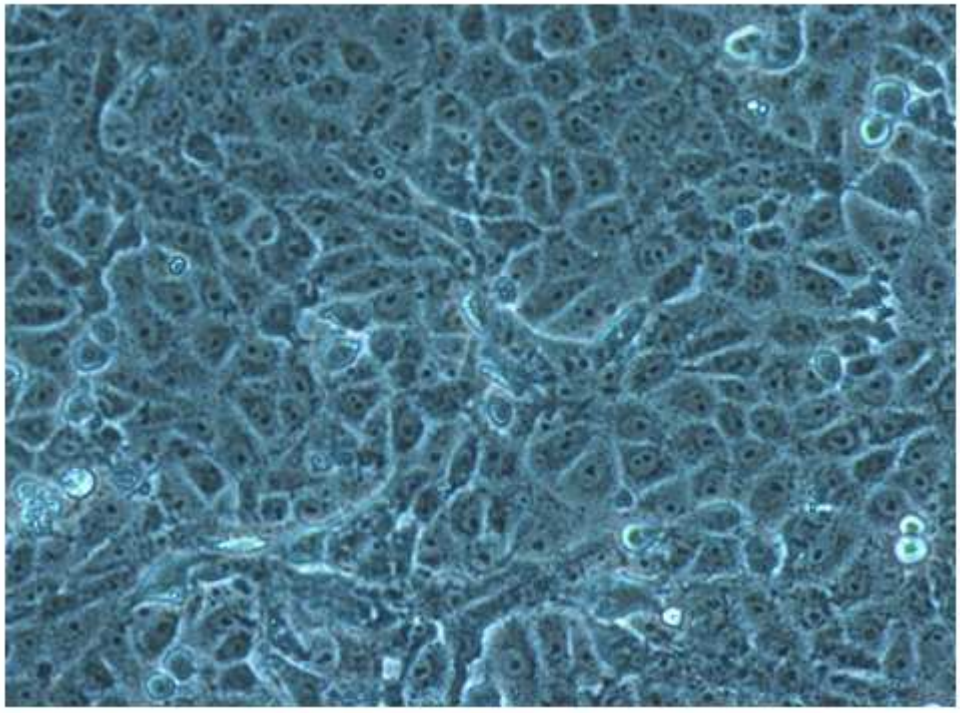

Silver Treated HepG2

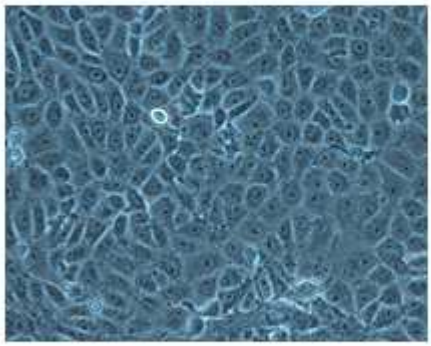

Figure (3B) HepG2 with of AgNPs Effect of AgNPs treatment on HepG2 cells. Light microscopy (phase contrast, 40x) 24 hours exposure to 10µM (low dose) AgNPs.

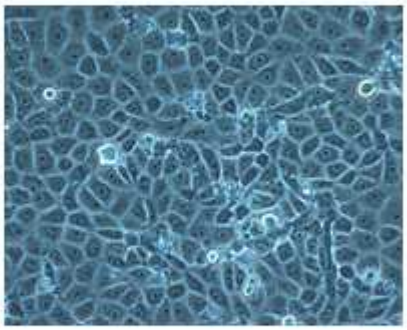

Figure (3C) Effect of AgNPs treatment on HepG2 cells. Light microscopy (phase contrast, 40x) 24 hours exposure to 100 µM (high dose) AgNPs.

Gold Treated HepG2

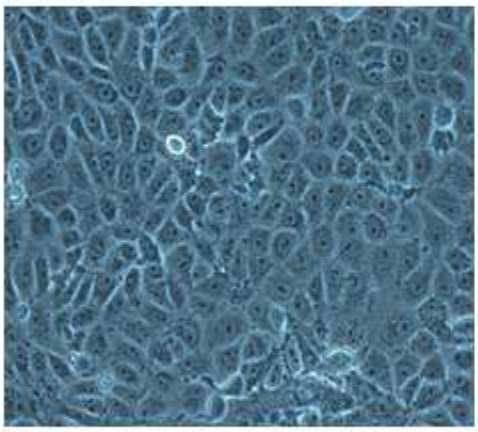

Figure (3D) HepG2 with of AuNPs Effect of AgNPs treatment on HepG2 cells. Light microscopy (phase contrast, 40x) 24 hours exposure to 10µM (low dose) AuNPs.

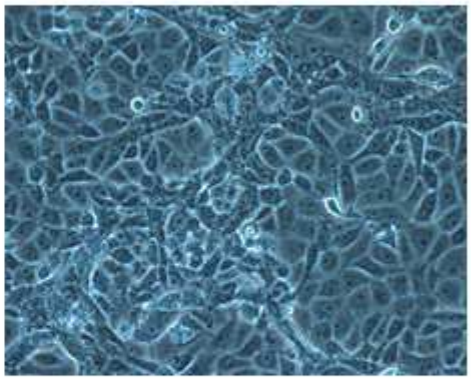

Figure (3E) Effect of AuNPs treatment on HepG2 cells. Light microscopy (phase contrast, 40x) 24 hours exposure to 100 µM (high dose) AuNPs.

Table 4. Genomic DNA content of DNA fragmentation assay after treatment of cells with AgNPs

Sample	Conc ng/µl	Ratio (260/280)
Au low conc (10 µM)	67.5	1.86
Au high conc (100 µM)	40	1.75
Control (untreated HepG-2)	69	1.85

Figure 4A. HepG2 cells by transmission electron microscope
Indicated : N (nucleus), NM (nuclear membrane), CM (cell membrane),
Ch (chromatin), Cyto (cytoplasm)

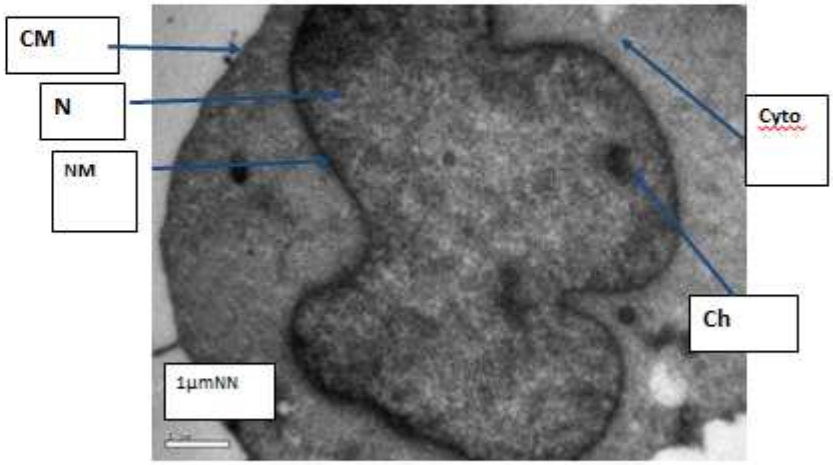

Fig ( ) TEM images of untreated (control) HepG2, with a magnification of 15000 times

Figure 4A. HepG-2 cells by transmission electron microscope
Indicated : N (nucleus), NM (nuclear membrane), CM (cell membrane),
Ch (chromatin), Cyto (cytoplasm)

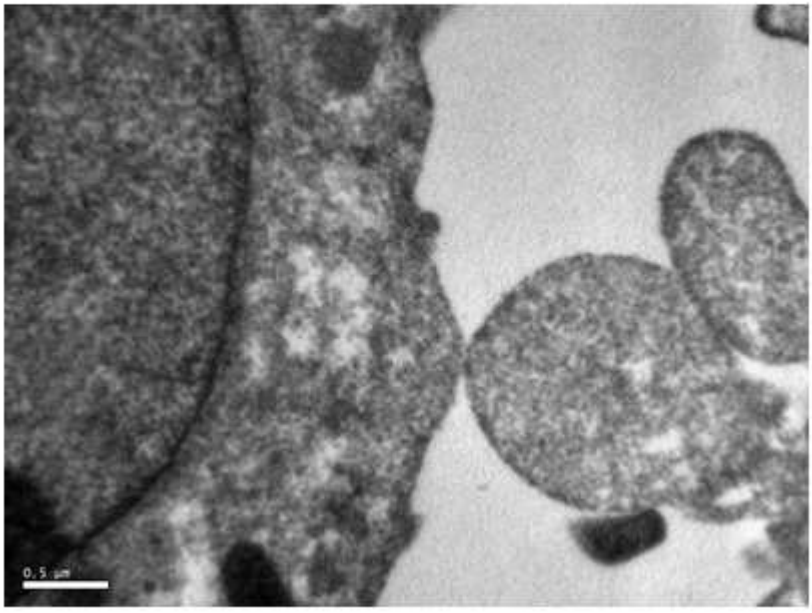

TEM images of untreated (control) HepG2, with a magnification of 30000 times

Figure 4 B . TEM images of AgNPs treated HepG2, with a magnification of 30000 times.

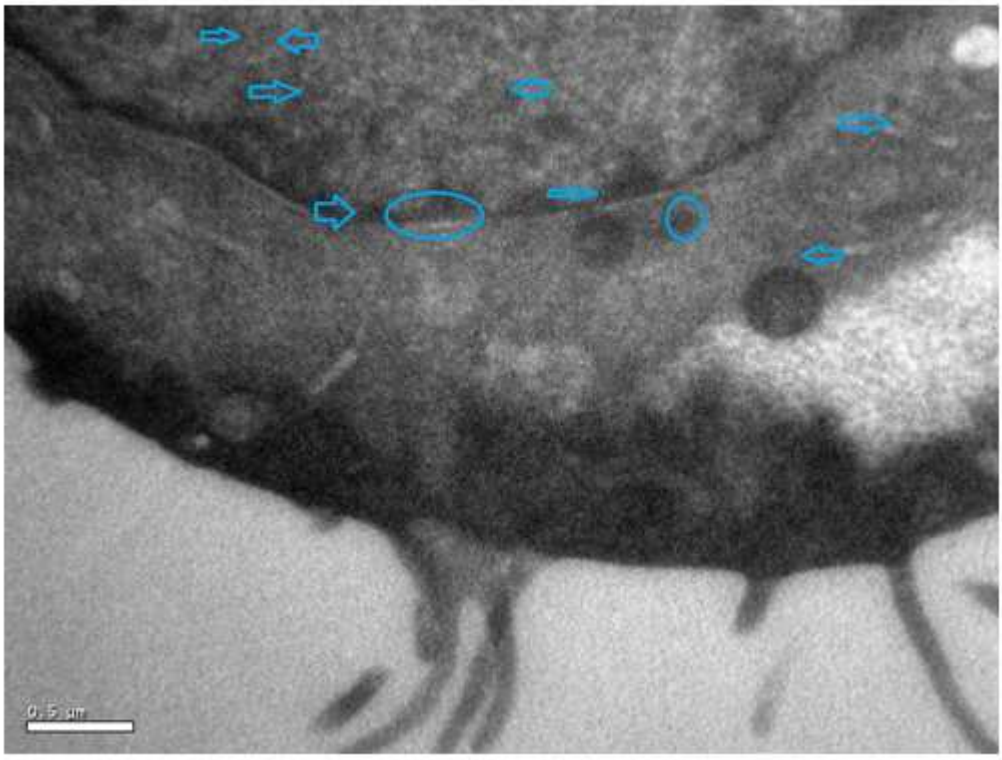

Figure 4 C. TEM images of AuNPs treated HepG2, with a magnification of 30000 times

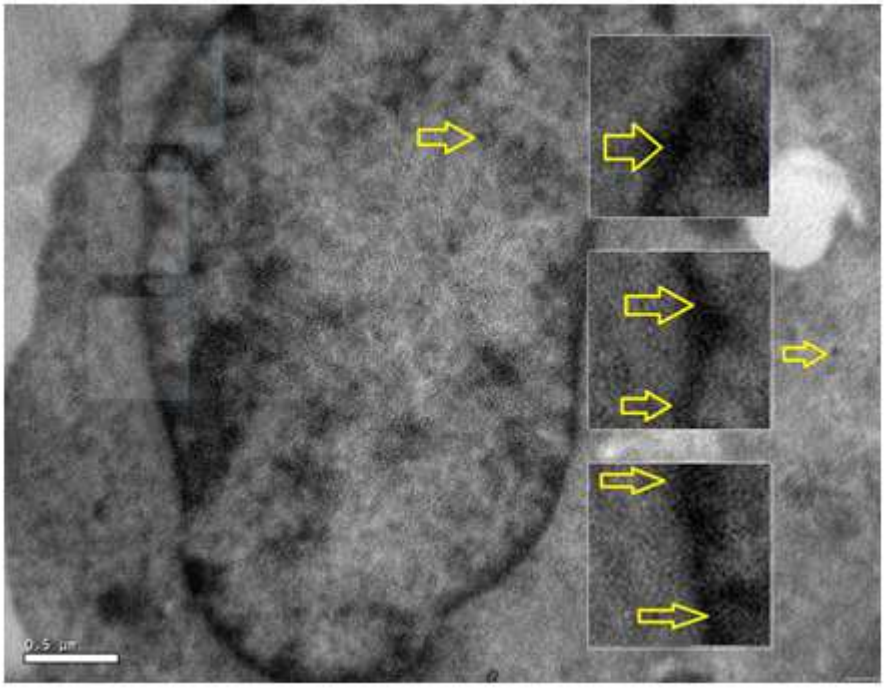

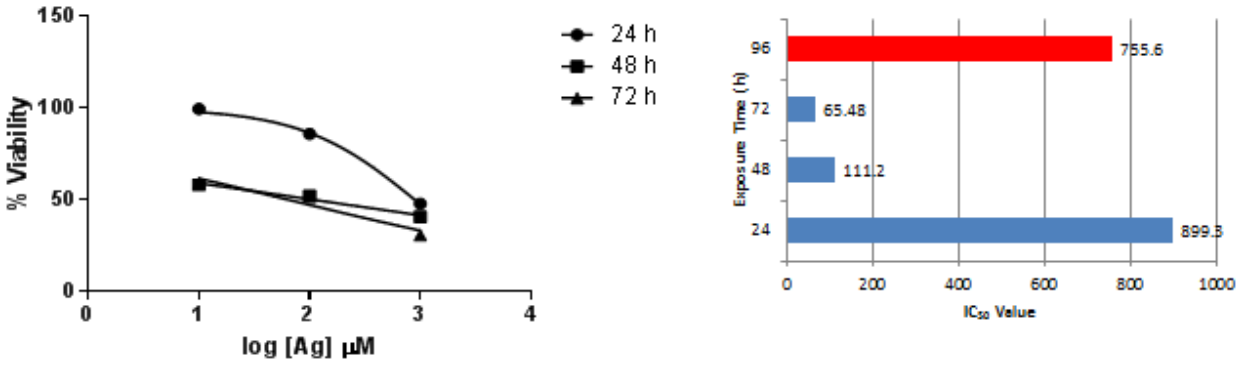

Figure 5 A.

Figure 5B. Concentration dependence of AuNPs on HepG-2 cells, as detected by SRB assay after48hrs of cell exposure

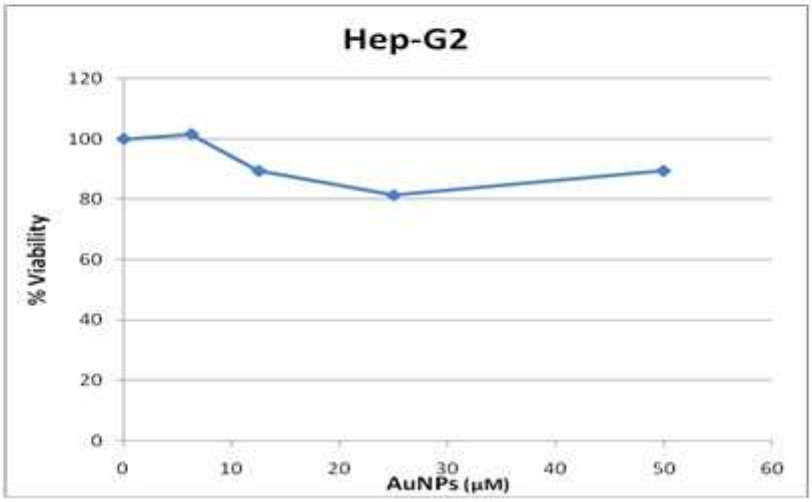

Table 6. Primers used for apoptotic genes expression

Caspase-3	399 bp	399 bp	Forward: 5_-TTTGTTTGTGTGCTTCTGAGCC-3_
			Reverse: 5_-ATTCTGTTGCCACCTTTCGG-3_
Bak	1056 bp	1056 bp	Forward: 5_-TCCAGATGCCGGGAATGCACTGACG-3_
			Reverse: 5_-TGGTGGGAATGGGCTCTCACAAGG-3_
P53	540 bp	540 bp	Forward: 5_-TGGCCCCTCCTCAGCATCTTAT-3_
			Reverse: 5_-GTTGGGCAGTGCTCGCTTAGTG-3_
Bax	326 bp	326 bp	Forward: 5_-AAGCTGAGCGAGTGTCTCAAGCGC-3_
			Reverse: 5_-TCCCGCCACAAAGATGGTCACG-3_

Figure. 6A. Flow cytometric analysis, shows four distinct phases could be recognized in a proliferating cell population: the G1-, S-(DNA synthesis phase), G2- and M-phase (mitosis). However, G2- and M-phase, which both have an identical DNA content, could not be discriminated based on their differences in DNA content. 50µM of AgNPs

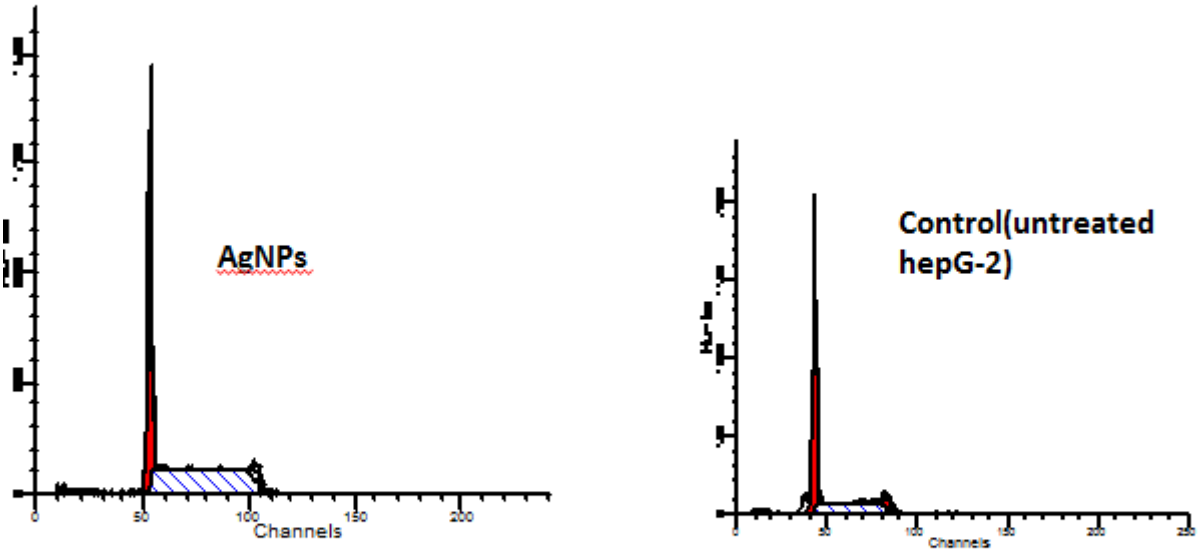

The silver nanoparticles treatment of HepG2 cell line caused diploid cells of 100% to be arrested in G0/G1 phase by about 52.12 %, and G2/M: 3.05 % while S phase was arrested by about 44.83 %, the G2/G1 phase: 1.94%, diagram.

Figure 6B. Flow cytometric analysis, shows four distinct phases could be recognized in a proliferating cell population: the G1-, S-(DNA synthesis phase), G2- and M-phase (mitosis). However, G2- and M-phase, which both have an identical DNA content, could not be discriminated based on their differences in DNA content. 50µM of AuNPs

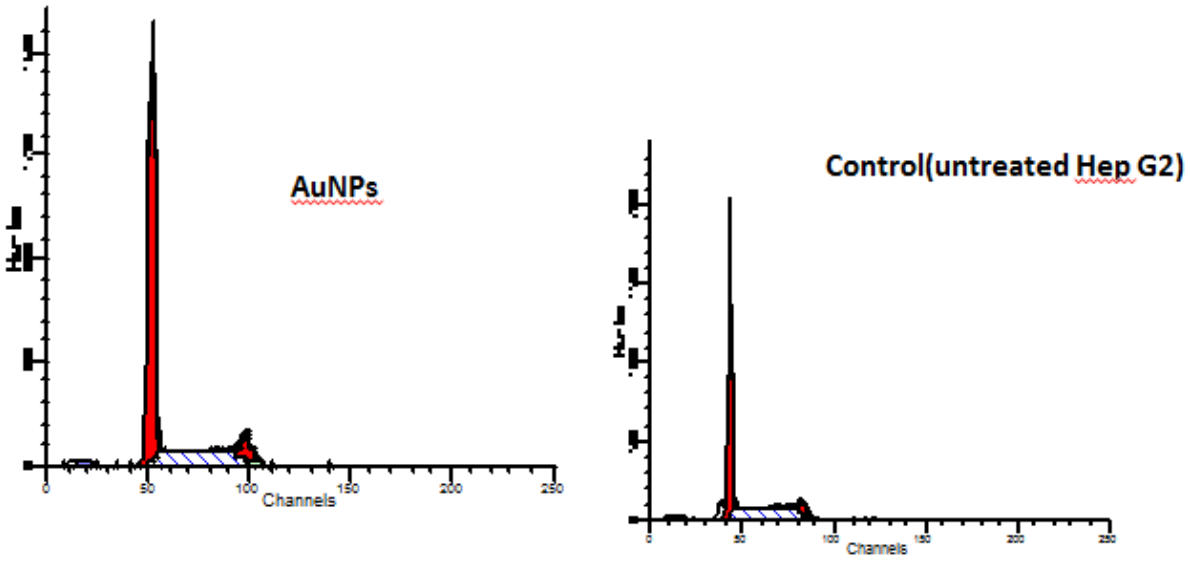

The gold nanoparticles treatment of HepG2 caused diploid cells of 100% to be arrested in G0/G1 phase by about 70.52 %, and G2/M: 8.54 % while S phase: 20.94 % the G2/G1 phase: 1.91%, diagram ( ).

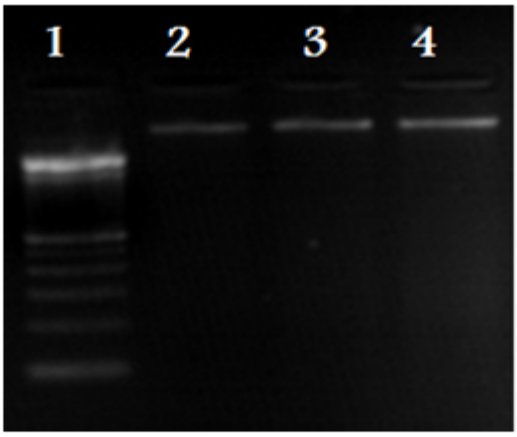

Figure 7A. EB-stained gel electrophoresis of genomic DNA extraction at conc. of 150ng from untreated and treated Hepg2 cell line with different concentrations of **AgNPs**. Lane 2 (treated cells with 10 µM/ml), Lane 3 (treated cells with 100 µM/ml), lane 4 untreated Hepg2 (cell control), and 100 bp ladder in lane 1.

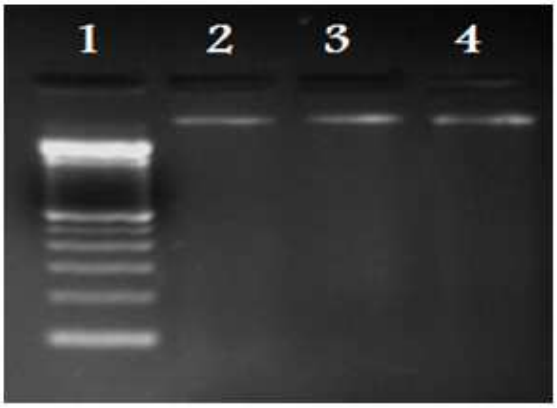

Figure 7B. EB-stained gel electrophoresis of genomic DNA extraction from untreated and treated HepG-2 cell line with different concentrations of **AuNPs**. Lane 2 (Hep-2 with 100 µM/ml), Lane Lane3 (treated HepG-2 with 10µM/ml), lane 4 untreated Hepg-2 (cell control), and 100 bp ladder in lane 1

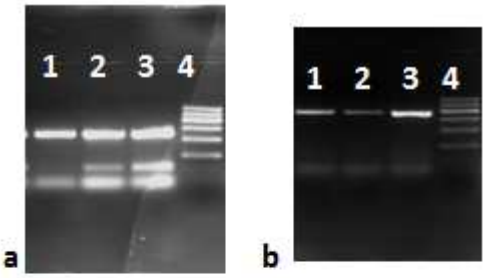

Figure 8A. EB-stained gel electrophoresis of genomic **β actin** RNA house keeping gene from untreated and treated HepG2, Lane 1: Untreated HepG2, Lane 2: HepG2 treated with 100µAuNPs, Lane 3 : HepG2 treated with 100µM AgNPs (253bp)

Figure 8 B. EB-stained gel electrophoresis of genomic **P53** RNA expression from untreated and treated HepG2, Lane 1: Untreated HepG2, Lane 2: HepG2 treated with 100µAuNPs, Lane 3 : HepG2 treated with 100µM AgNPs 366 bp

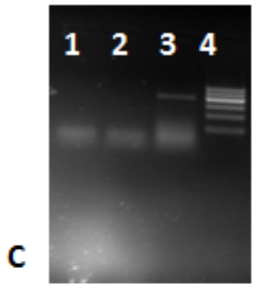

C

Figure 8 C. EB-stained gel electrophoresis of genomic **Caspase 3** RNA expression from untreated and treated HepG2, Lane 1: treated HepG2d with 100µAuNPs, Lane 2 : HepG2 treated with AgNPs, Lane 3 : untreated cells, Lane 4 : 100 bp ladder, Caspase at 399 bp

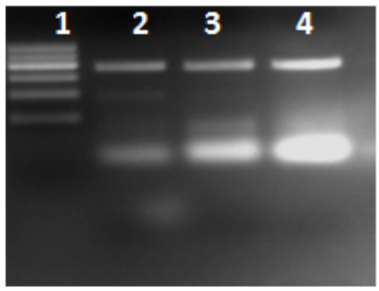

D

Figure 8D. EB-stained gel electrophoresis of genomic **BCL2** RNA expression from untreated and treated HepG2, Lane 2: Untreated HepG2, Lane 3: HepG2 treated with 100µAuNPs, Lane 4 : HepG2 treated with 100µM AgNPs , lane 1 is 100 bp ladder,
BCl2 at 366 bp

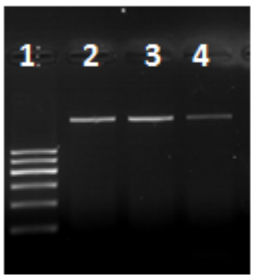

E

Figure 8 E. EB-stained gel electrophoresis of genomic **BAK** RNA expression from untreated and treated HepG2, Lane 2: Untreated HepG2, Lane 3: HepG2 treated with 100µAuNPs, Lane 4 : HepG2 treated with 100µM AgNPs , lane 1 is 100 bp ladder,
BAK at 1056 bp

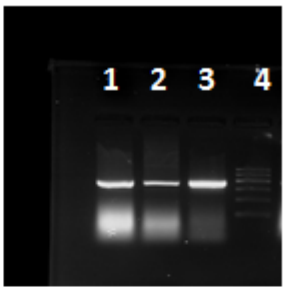

F

Figure 8 F. EB-stained gel electrophoresis of genomic **BAX** RNA expression from untreated and treated HepG2, Lane 1: Untreated HepG2, Lane 2: HepG2 treated with 100µAuNPs, Lane 3 : HepG2 treated with 100µM AgNPs , lane 1 is 100 bp ladder,
BAX at 326 bp

DISCUSSION

Previous studies have demonstrated biomedical applications of metallic nanoparticles especially as antimicrobial and antitumor activities [21]. In the current study HepG2 in vitro model of human liver cancer cells [22] was used because this disease is considered one of the commonest cancer diseases among Egyptian population, and is often fatal. The available traditional treatment is not effective and subjected to resistance; therefore there is a need to newer treatment approaches.

However several studies have shown that metallic nanoparticles may induce genotoxicity and cytotoxicity in cancer and normal cell lines and they emphasized their role in cancer therapy [23,24,25] most of them have demonstrated fragmentary and conflicting results when explaining apoptotic mechanisms [26]. This was due to the non

homogeneity of the studies in terms of physicochemical properties of nanomaterials and experimental methods used for their preparation and type of cells [8]. It has been reported that the physicochemical properties of nanoparticles control all interactions of nanoparticles with the biological environment such as: activation of cellular stress-dependent signaling pathways, direct damage of sub-cellular organelles such as mitochondria and DNA fragmentation in the nucleus, resulting in cell cycle apoptosis, and inflammatory response [27,28]. Therefore, we found it is quiet relevant to have some knowledge about mechanistic basis of cytotoxic effect of our engineered metallic nanoparticles (AgNPs & AuNPs) in HepG2 cell line on a cellular and molecular levels before starting in vivo assay. This has been performed by investigating qualitative fragmentation of HepG2 DNA, microscopic imaging followed cell cycle analysis and some of apoptotic genes mRNA expression after 24 h of cell exposure. In our previous study, we have established in vitro neutral red colorimetric assay that can investigate cytotoxic effect of our engineered nanomaterials which was based on the ability of viable cells to incorporate and bind neutral red (NR). A weak cationic supravital dye penetrates cell membranes by non-ionic diffusion and accumulates in lysosomes. Any alterations in the cell surface or lysosomal membrane that lead to lysosomal fragility result in several changes. Such changes cause decreasing in binding of NR, permitting differentiation between viable, damaged, or dead cells via spectrophotometric measurements [16].

Concerning silver nanoparticles, our results showed that antiproliferative activity of such spherical nanoparticles at size of 22 nm and at different concentrations (10 µM, 100 µM and 1000 µM) increased by increasing time of exposure as evaluated by neutral red colorimetric assay. Also, our results showed that IC50 concentration was 111 µM (10.78 mg/L) after 48 h of cell exposure. Such effect was better than that previously reported by Kawata and his colleagues , who observed that treatment of HepG2 with AgNPs at size of 7-10 nm exhibited significant loss of viability at concentration of >1.0mg/L [29]. Their results support involvement of physicochemical properties as a crucial factor affecting cellular proliferation and hence antitumor activity. Our results was almost close to Lara and team work [30] but they used different types of cells, who reported that IC50 of AgNPs of 30-50 nm diameter was 1.11±0.32mg/ml against human PBMC, and 1.3±0.58mg/ml against MT-2 cells.

Regarding gold nanoparticles, our results showed that treatment of cells with such spherical nanoparticles at size of 36 nm and at concentration of 50 µM (15 mg/L) did not show much toxic effect (10%) by using SRB colorimetric assay which is more preferred than MTT assay [31]. When comparing cytotoxic effect among AgNPs and AuNPs, our results showed that AuNPs was safer on cells at the same concentration (50 µM) based on SRB colorimetric assay, This agreed with what has been reported regarding non toxic and biocompatibility of gold nanoparticles in vitro and in vivo [16]. But the conflicting cytotoxic results might be due to (1) inability of light microscopy to distinguish toxic effect of nanomaterials, (2) Possible interference of nanoparticles with dye molecules used in traditional colorimetric assay and (3) the cytotoxic effect obtained by colorimetric assay represents late event. Such reasons encouraged us, to perform further analysis at the cellular and molecular levels to analyze possible genotoxic effect of our engineered metallic nanoparticles. Our results revealed internalization of AgNPs and AuNPs in cellular organelles, cell membrane, cytoplasm, nucleus, mitochondria as shown by TEM.

Regarding cell cycle analysis, Austin and his colleagues have observed that interaction of nanosilver with DNA leads to cell cycle arrest at G2/M phase [32]. Moreover, it induced G1 arrest and completely blocks S phase, therefore inducing apoptosis [33,26]. This was almost in accordance with our results which showed progressive accumulation of cell population in the S phase correlating with decreased number of cells in the G2/M phase after treatment of cells with 100 µM of AgNPs for 24 h. Such results were also confirmed by results of cellular DNA fragmentation which showed lower concentration of cellular DNA extracted from treated cells compared to untreated one.

In our previous report, we have reviewed the possible factors linked to cytotoxic effect of AgNPs [16]. In addition to mitochondrial dysfunction, and ROS generation. McShan and his colleagues have found that treatment with nanosilver could induce the release of cytochrome c into the cytosol and subsequent translocation of Bax to the mitochondria, indicating that nanosilver acts through ROS and C-Jun N-terminal kinase to induce apoptosis via the mitochondrial pathway [33]. The close relationship between p53 activation and DNA damage makes p53 the molecular marker of choice for assessing genotoxicity. Ahmed and his coworkers have observed that treatment of mouse embryonic stem cells and mouse embryonic fibroblast with AgNPs increased the level of p53 protein expression within 4 h of cells exposure [34].

In the current study, our results showed that expression of mRNA of p53, BAX, BAK, BCl2 as well as β actin were observed in untreated and treated HepG2 cells after 24 h of cell exposure to AgNPs at concentration of 100 µM (10.78 mg/L). But, mRNA of caspase3 was not detected in the treated cells at the same time interval. This could be explained by the following,

(1) Splicing of caspase-3 produces a short isoform caspase-3s that antagonizes caspase-3 apoptotic activity [35]
(2) caspase independent pathway
(3) Results needed to be repeated after longer time of cell exposure,48 ,96hr on a quantitative level before reaching a final conclusion.

Regarding apoptotic effect of gold nanoparticles, AuNPs were previously reported to have no toxic effects [5], but others found that they induce apoptosis in certain cell types [36,5,37,38]. It has been observed that cellular uptake of gold nanoparticles depends on size, cell type , concentration and time of exposure [39].

our previous study (In press) showed that treatment of human breast cancer cells (MCF-7) with our engineered gold nanoparticles at size of 34 nm and at concentration of 5 mg/L was associated with increased cell population in the S phase of cell cycle and decrease in G2/M phase of cell cycle after 24 h of cell exposure and presence of cell population in sub G-1phase of cell cycle. In contrast, in the current study, where HepG2 was used for treatment of AuNPs at the same concentration and the same conditions, results showed accumulation of cell population in G0/G1 and in G2/M phases of cell cycle.

This was also observed in a study performed by Chaung and his colleagues [40] when comparing cytotoxicity results of AuNPs in different human cancer cells, they provided a strong evidence that AuNPs act through distinct mechanisms to affect physiological process in different cell types, depending on cellular context and genetic background, for example, AuNPs (size 10 nm x 41nm) and at concentration of 180 ng/ml, resulted in cell cycle delay in A549 (human lung adenocarcinma), whereas apoptotic cell death was observed in AGS (human gastric adenocarcinoma) cells. In their study they have found that ROS involved in AuNPs induced apoptotic cell death in AGS cells but played no significant role in cell delay mediated by AuNPs in A549 cells [40]. Regarding some apoptotic genes expression to have knowledge about behavior of hepG2 cells in response to our engineered AuNPs capped with citrate, we found the presence of mRNA expression of β actin, Bak, Bax, P53,Bcl2 without expression of caspase mRNA in treated cells. From such observations we speculated that the cytotoxic effect of our designed AuNPs may be through caspase independent pathway according to the following explanations.

(1) Gold nanoparticles can gain access into mitochondria and stimulate ROS (caspase independent apoptosis pathway) production via impairing electron transport chain, structural damage, activation of NADPH-like enzyme system, and depolarization of the mitochondrial membrane [41]. Many researchers have observed that some compounds showed to be accompanied by AIF (proapoptotic factors) production which can induce caspase independent apoptosis. ROS is also involved in such route as it can mediate poly (ADP-ribose) polymerase-1 (PARP-1) activation, and PARP-1 activation is necessary for AIF release from mitochondria.

(2) It has been observed that Au NPs of different size (5 nm and 15 nm) can induce inhibition of cell proliferation mediated by apoptosis, as well as chromosomal damage, aneuploidogenic events, DNA strand breaks, pyrimidines and purines oxidative lesions in human PBL and in a murine macrophage cell line [42].

(3) Mironava and colleagues have speculated that apoptotic effect of human dermal fibroblast exposed to different sizes of AuNPs resulted from the number of vacuoles present in the cells, which is probably the main factor that disrupts the cytoskeleton causing cell area contraction and decreases in motility [39]. Moreover, western blot analysis indicated the up regulation of mitochondrial apoptosis proteins such as Bax and p53, down regulation of Bcl-2 and cleavage of poly(ADP-ribose) polymerase (PARP) confirming mitochondrial apoptosis and hence cell cycle arrest at the G0/G1 phase [43].

(4) Roa and his colleagues have concluded that Glu-AuNPs could trigger activation of the CDK kinases leading to cell cycle acceleration in the G0/G1 phase and accumulation in the G2/M phase. This activation was accompanied by a striking sensitization to ionizing radiation, which may have clinical implications [44] such findings were close to our observation where HepG2 treated with our designed AuNPs showed accumulation of cell population in G0/G1 phase and in G2/M phase (8% versus 6% of untreated cells).

(5) It has been observed that Bax might be an important mediator of P53 dependent apoptosis. The ratio of Bax to BCl2 can determine survival or death of the cells [45]. They have shown that the level of P53 expression is important to determine the cellular responses such that low levels of p53 expression resulted only in cell cycle arrest, and high levels of expression induced apoptosis and they have concluded that P53 induced apoptosis via activation of Bax dependent pathway [46].

All previous explanations showed some anticancer activity of gold nanoparticles, but further analysis is required regarding AuNP size, morphology, functionalization, concentration and the cell types with the most significantly antitumor activity.

CONCLUSION

We conclude that our designed silver nanoparticles at size of 22 nm didn't reveal cytotoxic effect measured by colorimetric assay, but it exerted genotoxic effect as shown by cell cycle analysis and DNA fragmentation. We suggested that apoptotic effect was intrinsic apoptotic caspase independent pathway via mitochondrial dysfunction but further analysis on a quantitative level is still required to confirm our results before suggesting antitumor activity of our engineered silver nanoparticles against human liver cancer cells application. Also assessing other parameters like ROS production and time of cell exposure is still required.

Regarding AuNPs at size of 36nm, it did not play a pivotal role in determining cytotoxicity. In contrast, the size, cell type and time of exposure were fundamental factors in inducing genotoxicity. Our designed AuNPs affected HepG2 cells at G0/G1 and at G2/M phases of cell cycle, and exerted their apoptotic effect via caspase independent pathway but with different mechanism than that exerted by silver nanoparticles. Further quantitative analysis is required to interpret scientific mechanism of apoptotic effects according to levels of apoptotic genes expression reaching to final conclusion.

We expect that a better understanding of apoptotic mechanism of metallic nanoparticles will widen their biomedical applications. Our community is in bad need for structured data on genotoxicity and immunotoxicity of released nanomaterials before biomedical application.

Acknowledgements
Our sincere gratitude to the team group of Nanotechnology & Advanced Materials Central Lab, Agriculture Research Center, Giza, Egypt. Funding provided by National Cancer Institute-Cairo University.

REFERENCES

[1] A Flores; Ja Marrero. *Clin. Med. Insights. Oncol.*, **2014**, 8, 71–6.
[2] N Mokhtar; I Gouda; I Adel. Cancer pathology registry 2003-2004 and time trend analysis, 2nd Edition, *Dep. Pathol. NCI*, Cairo, **2007**; 55–67.
[3] H Salama; AR Zekri; M Zern; A Bahnassy; S Loutfy; S Shalaby; C Vigen; W Burke; M Mostafa; E Medhat; O Alfi; E Huttinger. *Cell Transplant.*, **2010**, 19(11), 1475-1486.
[4] L Zhang; FX Gu; JM Chan; AZ Wang; RS Langer; OC Farokhzad. *Clin Pharmacol Ther*, **2007**, 83(5), 761-769.
[5] HK Patra; S Banerjee; U Chaudhuri; P Lahiri; AK Dasgupta. *Nanomedicine*, **2007**, 3(2), 111–120.
[6] P Mukherjee; R Bhattacharya; N Bone; Y K Lee; C R Patra; S Wang; L Lu; C Secreto; PC Banerjee; MJ Yaszemski; NE Kay; D Mukhopadhyay. *J. Nanobiotechnology*, **2007**, 5(1), 1-13.
[7] W Liu; Y Wu; C Wang; HC Li; T Wang; CY Liao; L Cui; QF Zhou; B Yan; GB Jiang. *Nanotoxicology*, **2010**, 4(3), 319–330.
[8] D De Stefano; R Carnuccio; MC Maiuri. *J. Drug Deliv.*, **2012**, 2012, 167896
[9] G Métraux; C Mirkin. *Adv. Mater.*, **2005**, 17(4), 412–415.
[10] M Hayat. Colloidal gold: principles, methods, and applications, Elsevier Science and Technology Books, New Jerser, USA, **2012**; 484.
[11] J Liu; Y Lu. *Nat. Protoc.*, **2006**, 1(1): 246–52.
[12] MA Hayat. Colloidal Gold Principles, Methods, and Applications, vol. 1. Academic Press, San Diego, **1989**; 536.
[13] NJ Schmidt. Diagnostic Procedures for Viral, Rickettsial and Chlamydial Infections, 6th Edition, American Public Health Association, Washington DC, **1989**.
[14] P Skehan; R Storeng; D Scudiero; A Monks; J McMahon; D Vistica; JT Warren; H Bokesch; S Kenney; M. R. Boyd. *JNCI J. Natl. Cancer Inst.*, **1990**, 82(13), 1107–1112.
[15] E Borenfreund; Ja Puerner. *Toxicol. Lett.*, **1985**, 24(2–3), 119–124.
[16] SA Loutfy; MB Mohamed; NT Abdel-Ghani; N Al-Ansary; WA Abdulla; OM El-Borady; Y Hussein; MH Eldin. *J. Nanopharmaceutics Drug Deliv.*, **2013**, 1(2), 138–149.
[17] R Nunez. *Curr. Issues Mol. Biol.*, **2001**, 3(3), 67–70.
[18] ZJ Zhu, PS Ghosh; OR Miranda; RW Vachet; V. M. Rotello. *J. Am. Chem. Soc.*, **2008**, 130(43), 14139–43.
[19] P Gopinath; SK Gogoi; A Chattopadhyay; SS Ghosh. *Nanotechnology*, **2008**, 19(7), 075104.
[20] P Gopinath; SK Gogoi; P Sanpui; A Paul; A Chattopadhyay; SS Ghosh. *Colloids Surf. B. Biointerfaces*, **2010**, 77(2), 240–5.

[21] SR Satapathy; P Mohapatra; R Preet; D Das; B Sarkar; T Choudhuri; MD Wyatt; CN Kundu. *Nanomedicine (Lond).*, **2013**, 8(8), 1307–22.
[22] L Inbathamizh; TM Ponnu; EJ Mary. *J. Pharm. Res.*, **2013**, 6(1), 32–38.
[23] H ÇİFTÇİ; M TÜRK; U TAMER; S KARAHAN; Y MENEMEN, *TURKISH. J. Biol.*, **2013**, 37, 573–581.
[24] A Shawkey; M. Rabeh. *Advances in Life Science and Technology*, **2013**, 13, 60–71.
[25] M Kodiha; YM Wang; E Hutter; D Maysinger; U Stochaj. *Theranostics*, **2015**, 5(4), 357–70.
[26] YC Huang; YC Yang; KC Yang; H.-R Shieh; TY Wang; Y Hwu; YJ Chen. *Biomed Res. Int.*, **2014**, 2014, 182353.
[27] A Nel; T Xia; L Mädler; N Li. *Science*, **2006**, 311(5761), 622–7.
[28] L Shang; K Nienhaus; GU Nienhaus. *J. Nanobiotechnology*, **2014**, 12(1), 5.
[29] K Kawata; M Osawa; S Okabe. *Environ. Sci. Technol.*, **2009**, 43(15), 6046–6051.
[30] HH Lara; NV Ayala-Nuñez; L Ixtepan-Turrent; C Rodriguez-Padilla. *J. Nanobiotechnology*, **2010**, 8, 1.
[31] ME Samberg; SJ Oldenburg; Na Monteiro-Riviere. *Environ. Health Perspect.*, **2010**, 118(3), 407–13.
[32] LA Austin; B Kang; CW Yen; MA El-Sayed. *Bioconjug. Chem.*, **2011**, 22(11), 2324–2331.
[33] D McShan; PC Ray; H Yu. *J. food drug Anal.*, **2014**, 22(1), 116–27.
[34] M Ahamed; M Karns; M Goodson; J Rowe; SM Hussain; JJ Schlager; Y Hong. *Toxicol. Appl. Pharmacol.*, **2008**, 233(3), 404–10.
[35] F Végran; R Boidot; E Solary; S Lizard-Nacol. *PLoS One*, **2011**, 6(12), e29058.
[36] Y Pan; S Neuss; A Leifert; M Fischler; F Wen; U Simon; G Schmid; W Brandau; W Jahnen-Dechent. *Small* ,**2007**, 3:1941-1949
[37] C Freese; C Uboldi; MI Gibson; RE Unger; BB Weksler; Ia Romero; PO Couraud; CJ Kirkpatrick. *Part. Fibre Toxicol.*, **2012**, 9(1), 23.
[38] K Li; X Zhao; BK Hammer; S Du; Y Chen; E Engineering; U States. *ACS nano*, **2013**, 7 (11), 9664–9674.
[39] T Mironava; M Hadjiargyrou; M Simon; V Jurukovski; MH Rafailovich. *Nanotoxicology*, **2010**, 4(1), 120–37.
[40] SM Chuang; YH Lee; RY Liang; GD Roam; ZM Zeng; HF Tu; SK Wang; PJ Chueh. *Biochimica et Biophysica Acta (BBA)*, **2013**, 1830(10), 4960-4973.
[41] Z Hongmei. Apoptosis and Medicine, TB Ntuli (editor.), InTech, Chinese Academic of medical science, CC BY 3.0 license, **2012**; 3–22.
[42] S Di Bucchianico; MR Fabbrizi; S Cirillo; C Uboldi; D Gilliland; E Valsami-Jones; L Migliore. *Int. J. Nanomedicine*, **2014**, 9(1), 2191–204.
[43] D Choudhury; PL Xavier; K Chaudhari; R John; AK Dasgupta; T Pradeep; G Chakrabarti. *Nanoscale*, **2013**, 5(10), 4476–89.
[44] W Roa; X Zhang; L Guo; A Shaw; X Hu; Y Xiong; S Gulavita; S Patel; X Sun; J Chen; R Moore; JZ Xing. *Nanotechnology*, **2009**, 20(37), 375101.
[45] PBS Lai; TY Chi; GG Chen. *Apoptosis*, **2007**, 12(2), 387–93.
[46] J Adams; S. Cory. *Science*, **1998**, 281(8), 1322–1326.